# Preface

The 2008 spring meeting of the *Arbeitskreis Festkörperphysik* was held in Berlin between February 24 and 29, 2008 in conjunction with the 72. Annual Meeting of the *Deutsche Physikalische Gesellschaft*. It was the last spring meeting of the *Arbeitskreis Festkörperphysik* because in the meantime it changed its name to *Sektion kondensierte Materie* which better shows that it also includes soft materials and biological systems. Therefore, the next spring meeting in Dresden will be organized by the *Sektion kondensierte Materie* of the *Deutsche Physikalische Gesellschaft*. The number of participants of this year's meeting in Berlin exceeded 5600 and there were more than 4600 scientific contributions. With these numbers this meeting was the largest physics meeting in Europe and among the largest physics meetings in the world in 2008.

The present volume, 48 of the *Advances in Solid State Physics* contains the written version of a large number of the invited talks in Berlin and gives a nice overview of the present status of condensed matter physics. Low-dimensional systems are dominating the field and especially nanowires and quantum dots. In recent years one learned how to produce nanowires directly during a growth process. Therefore, a number of articles is related to such nanowires. In nanoparticles and quantum dots the dimensionality is further reduced and we learn more and more how to produce such systems and what effects result from the confinement in all three dimensions. Spin effects and magnetism is another important field of present day research in solid state physics. The third chapter covers this physics including an article about *graphene*. The growing interest into organic materials and biological systems is reflected in a large chapter of this book with the title *Organic Materials and Water*. The last chapters of this book cover aspects which range from dynamical effects to device physics and characterization tools.

Hannover, June 2008 *Rolf J. Haug*

# Growth Methods and Properties of High Purity III-V Nanowires by Molecular Beam Epitaxy

D. Spirkoska ⋆, C. Colombo *, M. Heiß *, M. Heigoldt, G. Abstreiter, and A. Fontcuberta i Morral

Walter Schottky Institut, Technische Universität München, Am Coulombwall 3, 85748 Garching, Germany
annafm@wsi.tum.de

**Abstract.** The synthesis and properties of catalyst-free III–V nanowires with MBE is reviewed. The two main methods are Selective Area Epitaxy and gallium-assisted synthesis. The growth mechanisms are reviewed, along with the design possibilities of each technique. Finally, the excellent structure and ultra-high purity are presented by Raman and Photoluminescence spectroscopy.

## 1 Introduction

Semiconductor nanowires constitute extremely promising building blocks for the XXI century electronic and optoelectronic devices. One reason is that its size will enable further down scaling of electronics [1–3]. A second reason is that nanoscale objects exhibit new properties which at the same time can be exploited into new device concepts such as high mobility transistors, thermoelectric applications and/or solar cells [4–7]. As a consequence, fundamental and applied research on nanowires has increased dramatically in the last few years.

One issue of crucial importance has been the control on the crystalline quality and impurity concentrations, as well as the reproducibility of the structures. With regards to the purity, one of the key issues has been to avoid the use of gold as nucleation and growth seed of the nanowires. Gold is a fast-diffusing metal that significantly harms the properties of semiconductors [8]. To date, synthesis without gold has been achieved by the use of alternative metals such as aluminum and titanium, or by simply avoiding the use of a catalyst [9–12]. These alternative methods involve the development of new deposition techniques, meaning that the growth mechanisms necessarily differ from the standard Au-assisted VLS/VSS growth.

Traditionally, Molecular Beam Epitaxy (MBE) has been one of the oldest techniques applied to the fabrication of high quality nanostructures. Starting

⋆ Equal contribution

from Quantum Wells and Quantum Dots obtained by standard planar growth, the method has also been applied for the fabrication of quantum heterostructures extended in more dimensions [13]. In this paper, we study the possibilities that MBE gives us to fabricate high quality III–V As-based semiconductor nanowires, while avoiding the use of gold as seed for the nucleation. We will show how the use of MBE presents at the same time an additional interest, as this technique allows us to produce ultra-pure nanowires and quantum heterostructures on the nanowire facets with very high crystalline quality and atomically sharp interfaces. This new versatility of MBE in the growth of nanostructures opens great possibilities for the generation of novel devices with additional optical and electronic functionalities, as it has been previously shown in planar structures [14–16].

## 2 Experimental

The samples were grown in a high purity Gen-II MBE system. In all cases, two-inch GaAs wafers sputtered with a 10–60 nm thick silicon dioxide film were used as substrates. In the case of Selective Area Epitaxy, the oxide was patterned by combining lithography with reactive ion etching [17]. In the case of gallium assisted growth of nanowires, no patterning was realized on the surface. In order to ensure a contamination-free surface, prior to the introduction to the MBE chamber the substrates were dipped for 2 s in a buffered HF aqueous solution (10% HF). In order to desorb any remnant adsorbed molecules of the surface, the wafers were heated to 650°C for 30 min prior to growth. As a difference to standard nanowire growth, no external metal catalyst was used in any case for the growth of the nanostructures.

## 3 Selective area epitaxy

Selective Area Epitaxy (SAE) is one of the two techniques leading into the growth of nanowires with MBE, which at the same time avoids the use of gold as a nucleation seed and catalyst. The purpose of SAE is to restrict the incorporation of the adatoms to certain areas on a patterned substrate. Basically, the III–V substrate is masked with a patterned $SiO_2$ layer and growth conditions are appropriately chosen to restrict the epitaxial growth inside the apertures. This technique has both been used in Metalorganic Chemical Vapor Deposition (MOCVD) and MBE [11, 17–19]. In MOCVD the selectivity originates from a preferential decomposition of the metalorganic precursors in III–V surfaces with respect to the $SiO_2$. In the case of MBE, the selectivity originates from the lowering of the sticking coefficient of the species on the oxide, in comparison to the open III–V surfaces. Additionally, diffusion of adatoms from the oxide to the III–V windows plays a supplemental role.

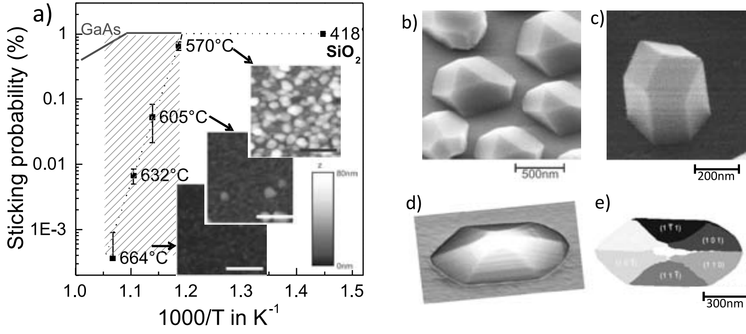


**Fig. 1.** (**a**) Measured sticking probability of GaAs on $SiO_2$ as a function of temperature, and comparison to literature values of the sticking probability on GaAs. In the inset, Atomic Force Micrographs of the surfaces after growth of 50 nm at the indicated temperatures. The scale bar stands for 400 nm. (**b,c**) Scanning Electron Micrograph of 200 nm GaAs grown by selective area epitaxy on (111)A and (111)B patterned substrates. (**d**) Atomic Force micrograph of 200 nm GaAs grown on (001) GaAs patterned substrate and (**e**) the corresponding attribution of the crystalline facets indexes.

We present first a study on the selective desorption of the Ga adatoms on surfaces by measuring the temperature dependence of the sticking coefficient, s, of GaAs on $SiO_2$. s is a measure of the probability of an adatom to precipitate forming a film instead of desorbing. It can be simply measured by comparing the nominal thickness with the actual thickness of material that has grown on the substrate. A nominal thickness of 50 nm GaAs was grown on $SiO_2$ at temperatures ranging between 418 and 664°C. The GaAs growth rate, as calibrated on GaAs at 550°C, was 0.4Å/s. The morphology of the surface after deposition was analyzed by Atomic Force Microscopy and Scanning Electron Microscopy (AFM and SEM respectively). In Fig. 1a, the results on the sticking coefficient of GaAs on $SiO_2$ ($s_{SiO_2}$) as a function of temperature are presented and compared to the literature values for GaAs on GaAs ($s_{GaAs}$) [20]. The AFM measurements of the surfaces after depositing nominally 50 nm of GaAs are also shown for illustration in the inset. For temperatures below 565°C , s is close to 1 in both cases meaning that 100% of the Ga adatoms precipitate on the oxide surface. For temperatures above 565°C, $s_{SiO_2}$ starts to decrease and stays well below the value on GaAs. This means that for these temperatures, the fraction $(1 - s)$ of Ga adatoms desorb from the surface. Finally, at temperatures higher than 650°C, s on $SiO_2$ is very close to zero, meaning that deposition of GaAs is not possible.

We have grown different thicknesses of GaAs on patterned substrates, at 650°C. Different substrate orientation has been used, in order to compare the morphology of the obtained structures. For deposited thicknesses below 100 nm, the growth in the openings occurs in a planar way and no significant difference is observed between the substrates. However, for higher nominal thicknesses the pillars develop clearly defined facets that are always defined in terms of minimization of energy. According to our results and the existing literature, the facets with the lowest formation energy are those of the family {110} and {111}, as well as sometimes 311. In Fig. 1b–d the scanning electron microscopy (SEM) and AFM measurements of structures grown by SAE on different substrates are shown. The substrates are in all cases GaAs, the only difference is the crystalline orientation of the substrate. In Fig. 1b and 1c, the SEM of structures grown on (111)A and (111)B patterned substrates are shown. Clearly the faceting geometry is significantly different. Due to the perpendicularity between (111)B and (1–10) facets, only in the case of (111)B substrates a vertical growth in the form of nanowire is possible. In the other cases, the faceting leads into pyramidal or multipolyhedral structures. Another example is given in Fig. 1d, where an Atomic Force micrograph of 200 nm GaAs grown on (001) GaAs patterned substrate is shown. The corresponding attribution of the crystalline facets indexes is shown in Fig. 1e. It should be noted here that faceting is not a new phenomenon in MBE growth. As an example, it has been known for a long time that self assembled Stranski-Krastanov quantum dots present high index facets of the type (110), (311)... [21]. The crystallographic orientation of the facets was investigated by detailed analysis of AFM measurements. We have observed that the facets correspond generally to the plane families {110} and {111}, which are known to be the crystal facets in III–V semiconductors with the lowest energy [22, 23]. As a conclusion, minimization of surface energy and faceting is a general effect in the nearly equilibrium growth of nanostructures, faceting depends on the crystal orientation of the substrate. Here we would like to add that faceting can add degrees of freedom in the design of functional heterostructures. Heterostructures grown on faceted nanopillars will offer the possibility of in situ growing kinked quantum wells with MBE [17]. Indeed, at the interface of two or three kinked quantum wells, the existence of further confined states such as quantum wires and dots are expected, as it has been observed before by MOCVD [18]. The position of these quantum wires and dots are predetermined by the previous pattern and therefore offer many new possibilities of design for nanoscale devices.

The main advantages of SAE are the control at the monolayer level and the possible use of faceting for the exploring of additional quantum heterostructures. A drawback of SAE is the slow growth rate of the structures. For SAE to occur, high temperatures are important but also low arrival rate of the

group III adatoms. This low growth rate does not allow the fabrication of high aspect ratio structures.

## 4 Conditions leading to group III assisted growth of nanowires

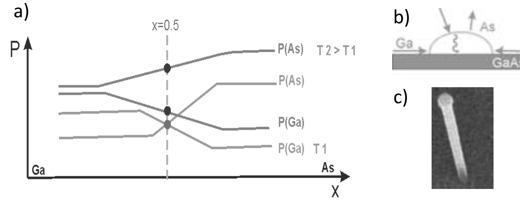


**Fig. 2.** (**a**) Vapor pressure schematic dependence of $Ga_{1-x}As_x$ for T1 below the congruent temperature and T2 above the congruent temperature (**b**) Schematics of the equilibrium of a Ga droplet on a GaAs substrate at Ga-rich conditions, above the congruent temperature and (**c**) Scanning electron micrograph of a 500 nm long GaAs nanowire grown under conditions of (**b**). The Ga droplet is observed on the top of the nanowire grown on a $SiO_2$ coated GaAs substrate.

A fundamentally different method to obtain III–V nanowires is based in the Vapor–Liquid–Solid method, in which a metal droplet is used to gather and precipitate the growth precursors. Typically, gold is a metal that works relatively well for any material. Instead, in principle it should possible to use group III metal droplets to gather group V elements and precipitate III–V nanowires underneath. In the case of GaAs nanowires, this leads to what we call "*gallium assisted growth*"; but the method can be extended to other III–V combinations such as InAs, InGaAs and AlAs .... For simplicity, we will just discuss the case of GaAs and therefore name these conditions as Ga-rich. In order to find the right conditions, it is necessary to look at the gallium and arsenic partial pressures of GaAs as a function of temperature. A schematics of this diagram is shown in Fig. 2 [24, 25]. For temperatures below 630°C the vapor pressures of Ga and As lead to a congruent evaporation of atoms, meaning that the evaporation rate of Ga and As is the same. At higher temperatures, this balance is not possible because the partial pressure of As is higher. In practice, this leads to the selective evaporation of As which in turns results in the formation of Ga droplets at the surface. This transition temperature is commonly referred as congruent temperature [24]. In order to use these Ga droplets for the gathering of As and growth of GaAs nanowires, a further element has to be considered. Indeed, in order to avoid the spreading and increase of the Ga dropet, it is necessary to avoid the wetting of the

metal on the surface. For this reason, GaAs surface has to be avoided. We have proved that this purpose can be reached covering the GaAs substrate with a thin $SiO_2$ layer.

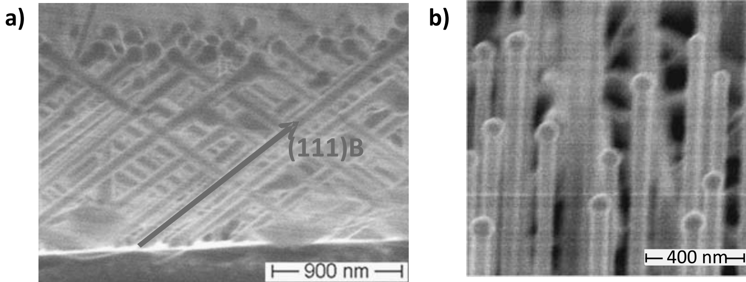


**Fig. 3.** (**a**) Scanning electron micrograph (SEM) of GaAs nanowires grown on a $SiO_2$ coated GaAs substrate. The substrate surface is (001), leading into the growth of GaAs wires on a 34° angle, which coincides with the (111)B crystalline direction of the substrate. (**b**) SEM of nanowires grown on a (111)B oriented substrate.

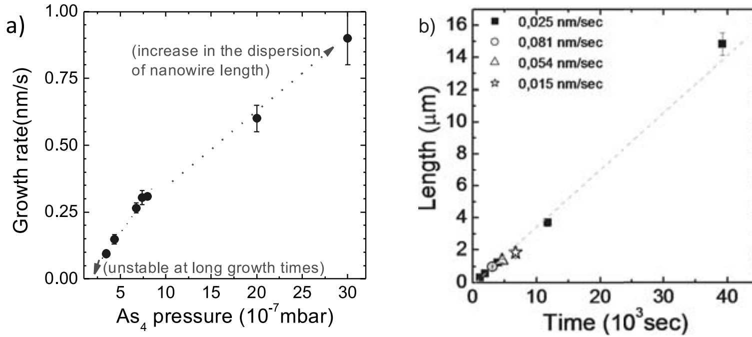


**Fig. 4.** (**a**) The growth rate of the GaAs nanowires tends to increase linearly as a function of the $As_4$ beam pressure. For pressures below $3 \cdot 10^{-7}$ mbar, the growth rate diminishes abruptly and the growth is not stable. For pressures above $8 \cdot 10^{-7}$ mbar the length dispersion from wire to wire is much higher. (**b**) The length of the GaAs nanowires as a function of time for different Ga arrival rates, for an $As_4$ beam pressure of $8 \cdot 10^{-7}$ mbar. The nanowire growth rate seems to be Ga rate independent.

We have observed, that when the oxide is thin enough (below 30 nm), nanowires grow following the (111)B direction of the substrate [12]. This is shown in Fig. 3, where the SEM of nanowires grown on (001) and (111)B GaAs

substrates is shown. In one case, the wires grow forming a 34° angle with the surface, while in the other case the wires grow perpendicularly. In order to proof that the nanowire growth is governed by the arsenic, we investigated the effect of the arsenic beam flux on the growth rate of the GaAs nanowires. The results are shown in Fig. 4a. In agreement with our hypothesis, the growth rate is proportional to the arsenic beam flux in ranges from $3.5 \cdot 10^{-7}$ to $3.5 \cdot 10^{-6}$ mbar. For pressures below $3.5 \cdot 10^{-7}$ mbar, the growth rate is very low and the growth is highly unstable. Between 3.5 and $8 \cdot 10^{-7}$ mbar the dispersion in the nanowire growth rate is very small, while for higher beam pressures a large dispersion in the length exists. The reason for the increased size dispersion remains unclear, though one reason could be delayed incubation times among the nanowires. The growth rate of nanowires was also measured as a function of the Ga rate. In Fig. 4b, the length of the nanowires as a function of time is plotted for different Ga rates, with an As Beam pressure of $8 \cdot 10^{-7}$ mbar. It is clear that all points fall in the same line, indicating an identical growth rate for the Ga rates varied from 0.12 to 0.82 Å/s. This result indicates that under these conditions the growth of the nanowires is not limited by the amount of Ga adatoms arriving at the surface, as it is usually the case in epitaxial growth of GaAs thin films [26].

## 5 Structural and optical properties

The structural properties of the GaAs nanowires were investigated by Raman spectroscopy. Prior to the measurements, bundles of nanowires were dispersed on a silicon substrate. The Raman experiments were performed at room temperature by using the 488 nm line from an $Ar^+$ laser, focused with a 50x microscope objective. The measurements were realized with low excitation power (0.5 mW), in order to avoid the heating of the sample. A typical Raman spectra of the nanowires is presented in Fig. 5a. The solid black line is the recorded data while the green lines are result from a multiple Lorentzian fit. The peak positioned at 268.7 $cm^{-1}$ can be attributed to scattering from TO phonon and the peak positioned at 292.2 $cm^{-1}$ is due to scattering from LO phonon. The TO and the LO peaks are symmetric and have very small FWHM (around 4 $cm^{-1}$). The peak positions correspond exactly with the position of the TO and the LO peaks measured on bulk (111) GaAs. The measured values for the peak positions and FWHM are a good indication that the synthesized wires have excellent structural quality, free of defects and stress, which further corroborates the advantage of using MBE.

A third peak positioned at the low frequency side from the LO phonon is also clearly observed. As previous studies have shown, this peak can be attributed to scattering from surface optical phonon (SO) [27, 28]. A simple experiment further proofs the surface related nature of this mode. The nanowires were embedded in a PMMA matrix and subsequently measured by Raman. As

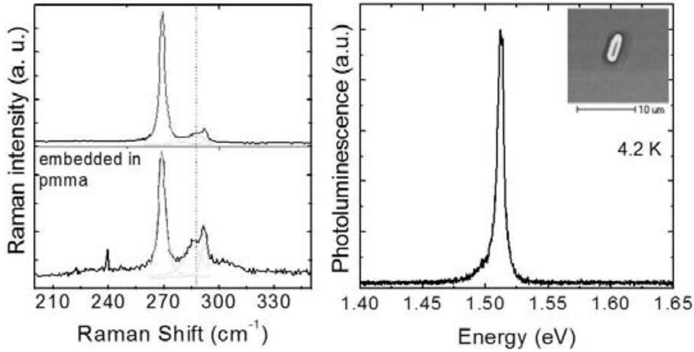


**Fig. 5.** (**a**) Raman spectroscopy on GaAs nanowires in air embedded in a PMMA matrix. The TO, LO and SO modes are indicated. As expected, the SO mode shifts when the wires are embedded in a matrix with a higher dielectric constant. (**b**) Photoluminescence spectroscopy on a single GaAs nanowire at 4.2 K. The small linewith corresponds well with the good crystalline quality. In the inset, an example of reflection scan realized on the sample surface to find the single nanowires.

predicted by the theory and shown in Fig. 5a, the increase in the surrounding dielectric constant leads into a shift of the SO mode, in this case of $1.8\,\mathrm{cm}^{-1}$.

In order to further assess the quality of the nanowires, photoluminescence spectroscopy (PL) on single nanowires was realized at 4.2 K, by means of a confocal microscope. The PL was excited using the 632.8 nm line of a He-Ne laser, and detected by the combination of a grating spectrometer and a silicon charge coupled device (CCD). For the measurements, the wires were dispersed on a silicon substrate. Scanning reflectivity measurements of the surfaces were realized in order to localize single nanowires. An example is shown in the inset of Fig. 5b, where the nanowire can be clearly identified in the middle of the scan. The PL emission of a single GaAs nanowire is shown in Fig. 5b. The PL spectrum is characterized by a peak centered at 1.51 eV with a full width at half-maximum of 6 meV, which corresponds well to the free exciton of undoped bulk GaAs. It should be stressed that these data are exceptional among the nanowires and further corroborate the high crystalline quality and purity of the nanowires. Here it is also important to note that the wires were not passivated, meaning that there might be very little surface states (which may be related to the fact that (110)GaAs surface has no band-gap states on the clean surface [29]). One should also note that we have observed that capped nanowires exhibit a PL higher in about a factor 100 with respect to the uncapped.

## 6 Potential for future structures and devices

We have shown in the previous sections, that MBE grown nanowires offer impressive structural and functional properties. At this moment it is open, the way they are going to play a significant role in the technology and basic science at the nanoscale. In this section, we would like to propose some of the future applications and perspectives of these wires.

The excellent properties of III–V materials are counterparted by their low abundancy – especially when compared with silicon – and the associated costs. For this reason, the combination of III–V semiconductors with the existing silicon-based technology has arised a great interest. This area of research has faced many challenges, mainly due to the lattice mismatch between the two materials. The problems and challenges associated with this can be overcome if the III–Vs are grown in the form of nanowire. Indeed, when the effective substrate area is reduced to the nanometer scale, the strain of the epilayer can relax laterally. The total strain energy of the system is reduced, enabling defect-free heteroepitaxy. The integration of III–V nanowires and related devices on silicon has already been shown in the past mainly by MOCVD and by using gold as a catalyst [30–32]. Catalyst-free MBE based growth of III-V nanowires on silicon still has to be demonstrated, but its achievement will bring the application of such materials much further in the technological path, as one could combine silicon technology with high performing III–V, densely packed vertical devices.

On another aspect, it is a matter of fact that the functionality of semiconductors augments significantly if dopant elements are incorporated in an efficient way. Dopants rule the conductivity of materials and allow the fabrication of devices like diodes, solar cells and transistors. Doping has been largely investigated and realized in a successful way for Si, GaN and ZnO nanowires, though theoretical works had predicted difficulties related to the diffusion of dopants towards the surface [33–37]. However, the controlled change of III–V nanowires' conductivity by doping has proven to be a difficult task. To our knowledge, highly efficient and controlled doping in the bottom-up approach of GaAs and InAs nanowires has been proved to be difficult, as dopants tend to not get incorporated during the growth process. As mentioned above, doping is key for advanced electronic and optoelectronic devices. For that, the intricate research on the synthesis, functional and structural characterization and theoretical understanding will be essential. At last, we will discuss a further advantage of MBE grown nanowires. Indeed, it is possible to switch the growth modus from nanowire-like to thin film-like. This enables the growth directly on the facets of the nanowires. This principle is indicated in Fig. 6a. Due to the directionality of the epitaxial beam, it is possible to grow on each of the facets or on the selected ones. Depending on the substrate used, the epitaxial growth will result in different geometries. For example, in the case the nanowires are grown on (111)B substrates, all layers have the same thickness. As a result, the cross-section of the layers forms a hexagon. This new design

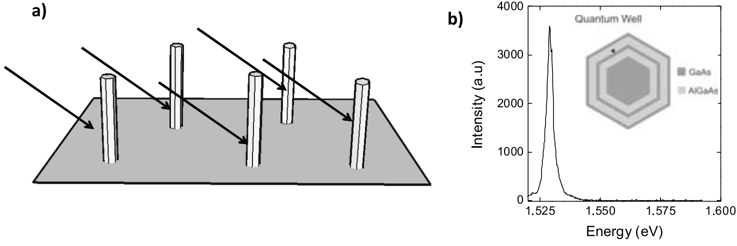


**Fig. 6.** (**a**) Schematics of the principle of heteroepitaxy on the facets of the nanowires. Due to the directionality of the beam, the geometry of the resulting layers results in hexagonal or asymmetric. Here, the geometry for nanowires grown on (111)B substrates is shown. (**b**) Photoluminescence of a 14 nm GaAs Quantum Well deposited on a nanowire.

possibility adds many new ways of adding functionality to the nanowires. With the purpose of proving this principle, a quantum heterostructure was grown on the {110} facets of wires grown on a (111)B substrate. The structure consisted of a quantum well (QW) of GaAs embedded in $Al_{0.3}Ga_{0.7}As$ barrier layers. The whole structure was capped with an thin layer of GaAs. The substrates were rotated at 7 rpm to ensure a uniform deposition. Thanks to the geometry of the nanowires, the deposition resulted in a prismatic configuration of the QWs, which we call p-QW. The selective growth on the {110} facets was achieved by increasing the $As_4$ beam flux to $5 \cdot 10^{-5}$ mbar, which is typical for 110 surfaces. Photoluminescence spectroscopy measurements were realized as a proof of principle. The spectrum is shown in Fig. 6b, where an unique emission peak centered at 1.53 eV is shown. This is consistent with a 14 nm quantum well, in agreement with the material deposited. Moreover, the same photoluminescence spectrum was obtained, when measured along the wire.

Coaxial-type nanowire heterostructures have been fabricated in the past. The function of the coating layer has been limited to the passivation of the surface states of the nanowires and has been fabricated with an isotropic radial morphology [38, 39]. Here we show that a uniform deposition on each side facets of a nanowire can be added with intrinsic functional purposes. Moreover, the lateral width of the QWs is in the order of 60 nm, meaning that the QWs pertaining to the prismatic structures can be considered as quasi one dimensional structures. The application of MBE to the fabrication of three dimensional quantum heterostructures opens a new avenue for a large variety of physical experiments and devices.

## 7 Conclusions

In conclusion, we have presented a novel method for growth of GaAs nanowires and prismatic quantum heterostructures by molecular beam epitaxy. We have presented and distinguished the method of selective area epitaxy and group III assisted growth. The two techniques avoid the use of gold for the nucleation and growth, solving the key issue of metal contamination. Moreover, we also show the advantages of using MBE which are: (1) a high purity leading into excellent structural and optical properties and (2) the selective growth of quantum heterostructures on the facets of the wires, providing a large new range of functionalities and applications.

## 8 Acknowledgements

The authors kindly thank D. Grundler, R. Gross, M. Stutzmann, J. R. Morante, M. Bichler and B. Laumer for experimental support and discussions. The financial support from Marie Curie Excellence Grant SENFED, Nanosystems Initiative Munich (NIM) and SFB 631 is greatly acknowledged.

## References

1. M. T. Björk, O. Hayden, H. Schmid, H. Riel, W. Riess: Vertical surround-gated silicon nanowire impact ionization field-effect transistors, Applied Physics Letters **90**, 142110 (2007) doi:10.1063/1.2720640
URL `http://link.aip.org/link/?APL/90/142110/1`
2. R. Chau, S. Datta, A. Majumdar: Opportunities and challenges of iii-v nanoelectronics for future high-speed, low-power logic applications, Compound Semiconductor Integrated Circuit Symposium, 2005. CSIC '05. IEEE SP-4 pp. (30 Oct.–2 Nov. 2005) doi:10.1109/CSICS.2005.1531740
3. J. Knoch, W. Riess, J. Appenzeller: Outperforming the conventional scaling rules in the quantum-capacitance limit, Electron Device Letters, IEEE **29**, 372–374 (April 2008) doi:10.1109/LED.2008.917816
4. W. Lu, J. Xiang, B. P. Timko, Y. Wu, C. M. Lieber: One-dimensional hole gas in germanium/silicon nanowire heterostructures, Proceedings of the National Academy of Sciences **102**, 10046–10051 (2005) doi:10.1073/pnas.0504581102
URL `http://www.pnas.org/cgi/content/abstract/102/29/10046`
5. A. Guichard, D. Barsic, S. Sharma, T. Kamins, M. Brongersma: Tunable light emission from quantum-confined excitons in tisi2-catalyzed silicon nanowires, Nano Letters **6**, 2140–2144 (2006)
URL `http://pubs3.acs.org/acs/journals/doilookup?in$_$doi=10.1021/nl061287m`
6. L. Shi, D. Li, C. Yu, W. Jang, D. Kim, Z. Yao, P. Kim, A. Majumdar: Measuring thermal and thermoelectric properties of one-dimensional nanostructures using a microfabricated device, Journal of Heat Transfer **125**, 881–888 (2003) doi:10.1115/1.1597619
URL `http://link.aip.org/link/?JHR/125/881/1`

7. J. Maiolo, B. Kayes, M. Filler, M. Putnam, M. Kelzenberg, H. Atwater, N. Lewis: High aspect ratio silicon wire array photoelectrochemical cells, Journal of the American Chemical Society **129**, 12346–12347 (2007)
URL `http://pubs3.acs.org/acs/journals/doilookup?in$_$doi=10.1021/ja074897c`
8. S. D. Brotherton, J. E. Lowther: Electron and hole capture at au and pt centers in silicon, Physical Review Letters **44**, 606–609 (1980) doi:10.1103/PhysRevLett.44.606
9. Y. Wang, V. Schmidt, S. Senz, U. Gosele: Epitaxial growth of silicon nanowires using an aluminium catalyst, Nature Nanotechnology **1**, 186–189 (2006)
URL `http://dx.doi.org/10.1038/nnano.2006.133`
10. T. I. Kamins, R. S. Williams, D. P. Basile, T. Hesjedal, J. S. Harris: Ti-catalyzed si nanowires by chemical vapor deposition: Microscopy and growth mechanisms, Journal of Applied Physics **89**, 1008–1016 (2001) doi:10.1063/1.1335640
URL `http://link.aip.org/link/?JAP/89/1008/1`
11. B. Mandl, J. Stangl, T. Martensson, A. Mikkelsen, J. Eriksson, L. Karlsson, G. Bauer, L. Samuelson, W. Seifert: Au-free epitaxial growth of inas nanowires, Nano Letters **6**, 1817–1821 (2006)
URL `http://pubs3.acs.org/acs/journals/doilookup?in$_$doi=10.1021/nl060452v`
12. A. F. i Morral, C. Colombo, G. Abstreiter, J. Arbiol, J. R. Morante: Nucleation mechanism of gallium-assisted molecular beam epitaxy growth of gallium arsenide nanowires, Applied Physics Letters **92**, 063112 (2008) doi:10.1063/1.2837191
URL `http://link.aip.org/link/?APL/92/063112/1`
13. G. Schedelbeck, W. Wegscheider, M. Bichler, G. Abstreiter: Coupled quantum dots fabricated by cleaved edge overgrowth: From artificial atoms to molecules, Science **278**, 1792–1795 (1997) doi:10.1126/science.278.5344.1792
URL `http://www.sciencemag.org/cgi/content/abstract/278/5344/1792`
14. K. Brunner, G. Abstreiter, G. Böhm, G. Tränkle, G. Weimann: Sharp-line photoluminescence and two-photon absorption of zero-dimensional biexcitons in a gaas/algaas structure, Physical Review Letters **73**, 1138–1141 (1994) doi:10.1103/PhysRevLett.73.1138
15. S. F. Fischer, G. Apetrii, U. Kunze, D. Schuh, G. Abstreiter: Energy spectroscopy of controlled coupled quantum-wire states, Nature Physics **2**, 91–96 (2006)
URL `http://dx.doi.org/10.1038/nphys205`
16. T. Egeler, G. Abstreiter, G. Weimann, T. Demel, D. Heitmann, P. Grambow, W. Schlapp: Anisotropic plasmon dispersion in a lateral quantum-wire superlattice, Physical Review Letters **65**, 1804–1807 (1990) doi:10.1103/PhysRevLett.65.1804
17. M. Heiß, E. Riedlberger, D. Spirkoska, M. Bichler, G. Abstreiter, A. F. i. Morral: Growth mechanisms and optical properties of gaas-based semiconductor microstructures by selective area epitaxy, Journal of Crystal Growth **310**, 1049–1056 (2008)
URL `http://www.sciencedirect.com/science/article/B6TJ6-4RHFVM6-1/1/b4df6ccca6568fdb6a0605ad3db318ab`

18. J. M. Hong, S. Wang, T. Sands, J. Washburn, J. D. Flood, J. L. Merz, T. Low: Selective-area epitaxy of gaas through silicon dioxide windows by molecular beam epitaxy, Applied Physics Letters **48**, 142–144 (1986) doi:10.1063/1.96977 URL http://link.aip.org/link/?APL/48/142/1
19. P. Mohan, J. Motohisa, T. Fukui: Controlled growth of highly uniform, axial/radial direction-defined, individually addressable inp nanowire arrays, Nanotechnology **16**, 2903–2907 (2005)
URL http://stacks.iop.org/0957-4484/16/2903
20. R. Fisher, J. Klem, J. T. Drummond, E. R. Thorne, W. Kopp, H. Morkoc, Y. A. Cho, *J Appl. Phys.* **54**, 2058–2510 (1983)
21. J. Márquez, L. Geelhaar, K. Jacobi: Atomically resolved structure of inas quantum dots, Applied Physics Letters **78**, 2309–2311 (2001) doi:10.1063/1.1365101 URL http://link.aip.org/link/?APL/78/2309/1
22. N. Moll, A. Kley, E. Pehlke, M. Scheffler: Gaas equilibrium crystal shape from first principles, Physical Review B **54**, 8844–8855 (1996) doi:10.1103/PhysRevB.54.8844
23. J. Márquez, P. Kratzer, L. Geelhaar, K. Jacobi, M. Scheffler: Atomic structure of the stoichiometric gaas(114) surface, Physical Review Letters **86**, 115–118 (2001) doi:10.1103/PhysRevLett.86.115
24. C. Chatillon, D. Chatain: Congruent vaporization of gaas(s) and stability of ga(l) droplets at the gaas(s) surface, Journal of Crystal Growth **151**, 91–101 (1995)
URL http://www.sciencedirect.com/science/article/B6TJ6-3Y5MNBT-CW/1/618e13e48368370025ebddc5476f2a8a
25. J.-y. Shen, C. Chatillon: Thermodynamic calculations of congruent vaporization in iii-v systems; applications to the in-as, ga-as and ga-in-as systems, Journal of Crystal Growth **106**, 543–552 (1990)
URL http://www.sciencedirect.com/science/article/B6TJ6-46D26H6-2C/1/61e6f54efa66285c41035fc80d35848d
26. C. Colombo, D. Spirkoska, M. Frimmer, G. Abstreiter, A. F. i Morral: Ga-assisted catalyst-free growth mechanism of gaas nanowires by molecular beam epitaxy, Physical Review B (Condensed Matter and Materials Physics) **77**, 155326 (2008) doi:10.1103/PhysRevB.77.155326
URL http://link.aps.org/abstract/PRB/v77/e155326
27. M. Watt, C. M. S. Torres, H. E. G. Arnot, S. P. Beaumont: Surface phonons in gaas cylinders, Semiconductor Science and Technology **5**, 285–290 (1990)
URL http://stacks.iop.org/0268-1242/5/285
28. D. Spirkoska, G. Abstreiter, A. F. i Morral: Size dependence of the bulk and surface phonon modes of gallium arsenide nanowires as measured by raman spectroscopy, Nanotechnology **19**, 435704 (2008)
29. J. Van Laar, J. J. Scheer: Influence of volume dope on fermi level position at gallium arsenide surfaces, Surface Science **8**, 342–356 (1967)
URL http://www.sciencedirect.com/science/article/B6TVX-46T3C5Y-29B/1/2da1fa525f4de8a02322ee95cea78ee0
30. T. Martensson, C. Svensson, B. Wacaser, M. Larsson, W. Seifert, K. Deppert, A. Gustafsson, L. Wallenberg, L. Samuelson: Epitaxial iii-v nanowires on silicon, Nano Letters **4**, 1987–1990 (2004)
URL http://pubs3.acs.org/acs/journals/doilookup?in$_$doi=10.1021/nl0487267

31. M. A. Sanchez-Garcia, E. Calleja, E. Monroy, F. J. Sanchez, F. Calle, E. Muñoz, R. Beresford: The effect of the iii/v ratio and substrate temperature on the morphology and properties of gan- and aln-layers grown by molecular beam epitaxy on si(1 1 1), Journal of Crystal Growth **183**, 23–30 (1998)
URL http://www.sciencedirect.com/science/article/B6TJ6-3W8STD4-4/1/ceb4d2577504cc8815a0de8507ed2712
32. L. Cerutti, J. Ristić, S. Fernández-Garrido, E. Calleja, A. Trampert, K. H. Ploog, S. Lazic, J. M. Calleja: Wurtzite gan nanocolumns grown on si(001) by molecular beam epitaxy, Applied Physics Letters **88**, 213114 (2006) doi:10.1063/1.2204836
URL http://link.aip.org/link/?APL/88/213114/1
33. Y. Cui, X. Duan, J. Hu, C. Lieber: Doping and electrical transport in silicon nanowires, Journal of Physical Chemistry B **104**, 5213–5216 (2000)
URL http://pubs3.acs.org/acs/journals/doilookup?in$_$doi=10.1021/jp0009305
34. K.-K. Lew, L. Pan, T. E. Bogart, S. M. Dilts, E. C. Dickey, J. M. Redwing, Y. Wang, M. Cabassi, T. S. Mayer, S. W. Novak: Structural and electrical properties of trimethylboron-doped silicon nanowires, Applied Physics Letters **85**, 3101–3103 (2004) doi:10.1063/1.1792800
URL http://link.aip.org/link/?APL/85/3101/1
35. S. Bae, C. Na, J. Kang, J. Park: Comparative structure and optical properties of ga-, in-, and sn-doped zno nanowires synthesized via thermal evaporation, Journal of Physical Chemistry B **109**, 2526–2531 (2005)
URL http://pubs3.acs.org/acs/journals/doilookup?in$_$doi=10.1021/jp0458708
36. G. Cheng, A. Kolmakov, Y. Zhang, M. Moskovits, R. Munden, M. A. Reed, G. Wang, D. Moses, J. Zhang: Current rectification in a single gan nanowire with a well-defined p–n junction, Applied Physics Letters **83**, 1578–1580 (2003) doi:10.1063/1.1604190
URL http://link.aip.org/link/?APL/83/1578/1
37. M. V. Fernández-Serra, C. Adessi, X. Blase: Surface segregation and backscattering in doped silicon nanowires, Physical Review Letters **96**, 166805 (2006) doi:10.1103/PhysRevLett.96.166805
URL http://link.aps.org/abstract/PRL/v96/e166805
38. N. Skold, L. Karlsson, M. Larsson, M.-E. Pistol, W. Seifert, J. Tragardh, L. Samuelson: Growth and optical properties of strained gaas-gaxin1-xp core-shell nanowires, Nano Letters **5**, 1943–1947 (2005)
URL http://pubs3.acs.org/acs/journals/doilookup?in$_$doi=10.1021/nl051304s
39. N. Skold, J. Wagner, G. Karlsson, T. Hernan, W. Seifert, M.-E. Pistol, L. Samuelson: Phase segregation in alinp shells on gaas nanowires, Nano Letters **6**, 2743–2747 (2006)
URL http://pubs3.acs.org/acs/journals/doilookup?in$_$doi=10.1021/nl061692d